Identification of Complex Karyotypes in Chronic Lymphocytic Leukemia: Comparison of Chromosome Banding Analysis and Genomic Microarray Techniques

Blanca Espinet[1,2]; Silvia Ramos[1,2]; Andrea Gómez-Llonín[1,2]; Sandrine Bougeon[3]; María José Calasanz[4]; Laura Blanco[5]; Rosa Collado[6]; Rocío Salgado[7]; María Ángeles Piñán[8]; Margarita Ortega[9]; María José Larráyoz[4]; Ana Batlle[10]; Andrea Campeny[11]; Alberto Valiente[12]; Eugènia Abella[1]; Eva Gimeno[1]; Pau Abrisqueta[9]; Félix Carbonell[6]; Carolina Moreno[5]; Francesc Bosch[9]; Ana Ferrer[1,2]; Marta Salido[1,2]; Gonzalo Blanco[1,2]; Jacqueline Schoumans3; Anna Puiggros[1,2]

[1] Laboratori de Citogenètica Molecular, Laboratori de Citologia Hematològica, Servei de Patologia i Servei Hematologia, Hospital del Mar, Barcelona, Spain.
[2] Grup de Recerca Translacional en Neoplàsies Hematològiques, Programa de Recerca en Càncer, Institut Hospital del Mar d'Investigacions Mèdiques (IMIM), Barcelona, Spain.
[3] Cancer Genetic Unit, Department of Clinical Hematology. Lausanne University Hospital, Lausanne, Switzerland. [4] Unidad de Citogenética y de Genética Hematológica, Departamento de Genética, Universidad de Navarra, Pamplona, Spain.
[5] Servei d'Hematologia Hospital Universitari de la Santa Creu i Sant Pau, Barcelona, Spain. [6] Servicio de Hematología, Consorcio Hospital General Universitario, Valencia, Spain.
[7] Laboratorio de Citogenética, Servicio de Hematología, Fundación Jiménez Díaz, Madrid, Spain. [8] Servicio de Hematología, Hospital de Cruces, Bilbao, Spain.
[9] Laboratorio de Citogenética y Servicio de Hematología, Hospital Vall d'Hebron, Barcelona, Spain. [10] Servicio de Hematología. Hospital Universitario Marqués de Valdecilla, Santander, Spain.
[11] Servicio de Hematología, Hospital San Pedro, Logroño, Spain. [12] Servicios de Genética y Hematología, Complejo Hospitalario de Navarra, Pamplona, Spain

Introduction

- Fluorescence *in situ* hybridization (FISH) assessment in chronic lymphocytic leukemia (CLL), analyzing del(13q), +12, del(11q)/*ATM* and del(17p)/*TP53*, underestimates true genomic complexity detected by either chromosome banding analysis (CBA) or genomic microarray techniques.
- Genomic complexity predicts an impaired outcome in CLL patients treated with standard or new treatments (ibrutinib, venetoclax).
- Complex karyotype (CK) has been defined as the presence of ≥3 abnormalities by CBA. Although it is the gold standard, CBA is not routinely performed in all centers.
- Genomic microarray techniques (CGH-array/SNP-array) are also capable to detect genomic complexity and do not require *in vitro* cultures, but no standard criteria to define CK by microarrays have been established.
- Consensus criteria to improve risk stratification based on genomic complexity are lacking.

Aim

1. To assess the complexity detected by genomic microarrays in patients with complex karyotype by CBA

2. To compare both methods regarding the number and type of aberrations detected in order to categorize patients based on genomic complexity

Patients and methods

- We included **57 CLL patients with complex karyotype by CBA**
  - Median age: 67; 70% males
  - Initial CLL stages → 67% Binet A
  - Median time from diagnosis to CBA/microarray analysis: 1 month (range, 0-137); 9/57 patients (15.8%) previously treated
  - The cohort was enriched in *ATM* deletion (22.2%) and *TP53* abnormalities (deletion and/or mutations) (43.4%)
- We compared the number, size and type of aberrations detected by:
  - CBA: at least ten metaphases from TPA-based cultures were analyzed to describe karyotypes following the 2016 ISCN nomenclature
  - Microarray analysis: DNA from peripheral blood mononuclear cells or CD19+ lymphocytes was hybridized to Cytogenetics Whole-Genome 2.7M array (n=2) or CytoScan HD array (n=55) (Affymetrix-ThermoFisher, Santa Clara, CA); results were analyzed with Chromosomal Analysis Suite Software

Contact: *bespinet@parcdesalutmar.cat*

Results

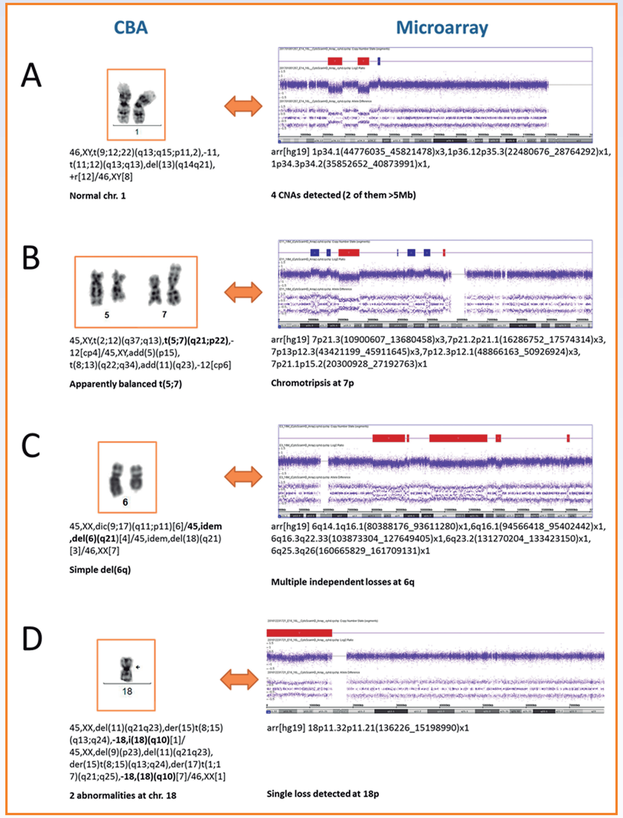

Figure 1. Examples of the discrepancies in the results obtained from both techniques. A) CNA >5Mb by microarrays in apparently normal regions by CBA; B & C) Higher complexity than initially described by CBA; D) Underestimation of abnormalities by microarrays

1. Overall results from both techniques:

- CBA identified a median of 4 aberrations (range: 3-19), being significantly lower than the copy number abnormalities (CNA) identified by microarrays (median 6, range: 0-29; P=0.009)
- The median size of the CNA detected by microarrays was 5.4Mb (range: 0.1-174Mb)

2. Comparison of different cut-off size to record CNA detected by microarrays for clinical interpretation (Figure 1):

- Application of current recommendations → only consider CLL known abnormalities and CNA >5Mb (Schoumans et al, 2016):
  - 42.7% of the initially detected CNA (179/419) were omitted
  - No significant differences in the number of abnormalities recorded by both techniques (P=0.334)

- Analysis of small CNA (≤5Mb) among the whole series:
  - **CNAs <1Mb:** did not involve any chromosomal altered region in the corresponding karyotype by CBA → their omission in the microarray assessment probably would not affect the stratification based on complexity
  - **CNA sized between 1 and 5Mb:**
    - Most of them involved some small CNA associated to apparently balanced translocations detected in the karyotype
    - In some cases revealed a higher genomic instability than the previously recognized by CBA (i.e. multiple deletions defined as a single deletion or a monosomy by CBA)

- Six cases showed **chromothripsis** involving small regions not detected by CBA which has been associated with impaired outcome in CLL (Salaverria et al, 2015)

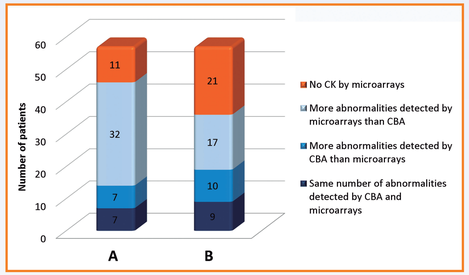

Figure 2. Comparison of the number of abnormalities detected by CBA and microarrays. A) Considering all the abnormalities by microarrays; B) Considering CLL known abnormalities and CNA >5Mb by microarrays (Schoumans et al, 2016)

3. Discrepancies of genomic complexity classification between both techniques:

- Genomic microarrays failed to detect some balanced translocations or subclonal aberrations by CBA, which probably were represented in a minor proportion of the sample but expanded during the TPA-based culture
- Eleven patients (19.3%) could only be considered complex by CBA (<3 CNA by microarrays), which increases up to 21 (37%) if current recommendations were applied **(Figure 2)**

Conclusions

1. The number of chromosomal abnormalities detected in CLL patients differs if assessed by CBA or genomic microarrays
2. The current 5Mb cut-off to define clinically relevant CNA should be revised, as it could underscore genomic instability (contiguous small deletions, chromothripsis)
3. More studies comparing chromosomal abnormalities detected by both techniques should be carried out to establish standard criteria for prognostic stratification of CLL patients based on genomic complexity consistent with the results from both techniques

Hospital del Mar

Parc de Salut MAR Barcelona

Clonal Relationship between Blastic Plasmacytoid Dendritic Cell Neoplasm and Myeloid Neoplasms

Luis Colomo, Concepción Fernández, Xavier Calvo, Blanca Espinet, Beatriz Bellosillo, Leonor Arenillas

Department of Pathology, Hematopathology Unit, Hospital del Mar-IMIM, Barcelona, Spain

Background

- Blastic Plasmacytoid Dendritic Cell Neoplasm (BPDCN) is an aggressive tumor derived from the precursors of plasmacytoid dendritic cells. BPDCN may associate with other myeloid neoplasm such as myelodysplastic syndromes (MDS), acute myeloid leukemia and chronic myelomonocytic leukemia (CMML).

Design

- We studied 5 patients with the concurrence of BPDCN and myeloid neoplasms (3 patients with MDS, and 2 CMML). All tumors were characterized by their cytological features, immunophenotype by flow cytometry (FC) and/or immunohistochemistry (IHC) and cytogenetics and targeted sequencing by NGS of genes recurrently mutated in myeloid malignancies.
- The panel of antibodies for FC and IHC included myeloid and B and T-cell lymphoid markers, as well as TdT, CD34, CD123, HLA-DR, and CD56 from Beckton Dickinson and Ventana; CD141 (BDCA-3), CD303 (BDCA-2), and CD304 (BDCA-4) were from Miltenyi Biotec. Cytogenetic studies included conventional karyotyping and FISH.
- Targeted sequencing of the whole codifying sequence of 51 genes recurrently mutated in myeloid malignancies was performed by NGS with the MiSeq sequencer, Illumina. The genes included were: *ABL1, ASXL1, ATRX, BCOR, BCORL1, CBL, CBLB, DAXX, DNMT3A, EED, ETV6, EZH2, FLT3, GATA1, GNAS, IDH1, IDH2, IKFZ1, JAK1, JAK2, JAK3, KAT6A, KIT, KRAS, MLL, MPL, NF1, NPM1, NRAS, PHF6, PRPF40B, PTPN11, RAD21, RB1, RUNX1, SETBP1, SF1, SF3A1, SF3B1, SH2B3, SMC1A, SMC3, SRSF2, STAG2, SUZ12, TET2, TP53, U2AF1, U2AF2, WT1* and *ZRSR2*.

Case #2; MDS 5q-, BM 2008

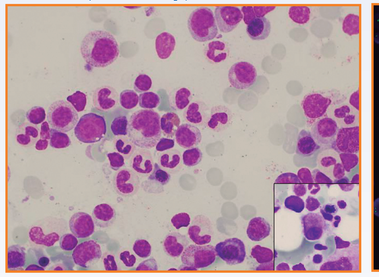

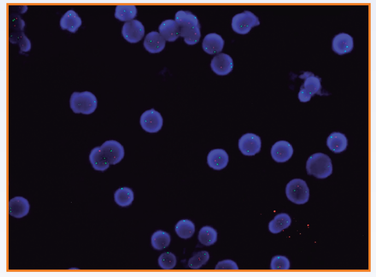

BPDCN, BM 2015

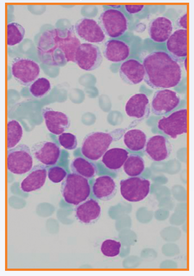

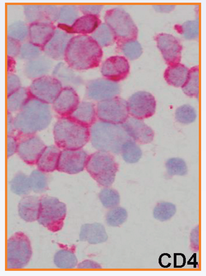

Case #3; CMML with trisomy 8, BM 2013

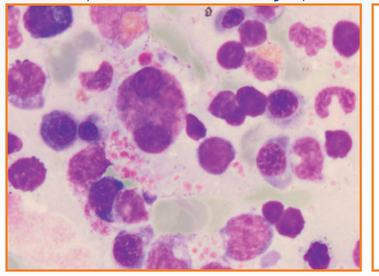

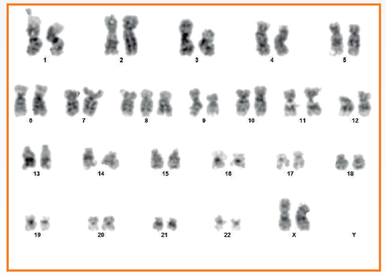

BPDCN, skin 2015

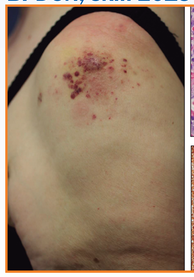

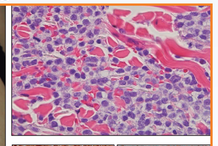

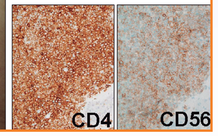

Results

- The patients were 3 males and 2 females with a median age of 74 years (range 61-82 years). BPDCN and MDS were synchronic in 2 cases (both patients diagnosed of refractory cytopenia with multilineage dysplasia), whereas BPDCN followed the myeloid neoplasms in 3 cases (1MDS with isolated del(5q), 2 CMML). All cases had involvement of the skin by BPDCN except for the case of MDS with isolated del(5q), that presented only with bone marrow involvement. In such case, del(5q) was also identified in the tumor cells of BPDCN. Trisomy 8 was identified in the tumor cells of either BPDCN and CMML in case #3.
- Results of targeted sequencing are showed in the table. Mutations in the splicing factors *ZRSR2* or *U2AF1* were observed in 3 cases, whereas no mutations were observed in either *SF3B1* or *SRSF2*, which are commonly mutated in MDS and CMML. As depicted in the table, the majority of mutations seen in the MDS/CMML phase were also observed when BPDCN appeared, with the exception of *TP53*, *IKZF1* and *NRAS* mutations that were only detected in BPDCN.

Case	Mutation	% MUT	% MUT
#1		**CMML, BM 2011**	**BPDCN, BM/skin 2013**
Male, 78 years	*TET2*: c.4468G>T; p.(Glu1490Ter)	40	35/40
	ZRSR2; c.868C>T; p.(Arg290Ter)	86	92/86
	ASXL1: c.1934dup; p.(Gly646TrpfsTer12)	18	31/0
	ASXL1: c.1900_1922del; p.(Glu635ArgfsTer15)	0	0/9
	IKZF1: c.610_638del; p.(Gly204LysfsTer7)	0	34/54
#2		**MDS 5q-, BM 2008**	**BPDCN, BM 2015**
Female, 82 years	*ASXL1*: c.1438G>T; p.(Glu480Ter)	38	49
	TET2: c.3466_3468del; p.(Asn1156del)	39	49
	TP53: c.536A>G; p.(His179Arg)	0	99
#3		**CMML, BM 2013**	**BPDCN, skin 2015**
Female, 82 years	*TET2*: c.2525C>G; p.(Ser842Ter)	42	90
	U2AF1: c.101C>T; p.(Ser34Phe)	43	46
	TET2: c.2428C>T; p.(Gln810Ter)	18	0
#4		**RCMD, BM 2013**	**BPDCN, skin 2015**
Male, 61 years	*TET2*: c.3263C>A; p.(Ser1088Ter)	21	42
	TET2: c.4122T>G; p.(Cys1374Trp)	19	39
	NRAS: c.182A>C; p.(Gln61Pro)	0	50
	ZRSR2: c.312G>A; p.(=) synonym, splicing site	21	91
#5		**RCMD, BM 2016**	**BPDCN, skin 2016**
Male, 70 years	*TET2*: c.1246_1247insCGAAC; p.(Pro416ArgfsTer13)	39	26
	KRAS: c.34G>T; p.(Gly12Cys)	3	53
	ASXL1: c.1934dup; p.(Gly646TrpfsTer12)	34	34

Conclusions

- These findings demonstrate a deferred clonal relationship between BPDCN and myeloid neoplasms in this series.
- Of note, all patients showed mutations in *TET2* implicating a probable impairment in the hidroxymethylation process. In addition, mutations involving tumor suppressor genes (*IKZF1* and *TP53*) and oncogenes (*NRAS* and *KRAS*) seem to have a triggering role for the development of the BDPCN.

Hospital del Mar

Parc de Salut MAR Barcelona

Review of the minimum immunostaining criteria for HER2 determination in gastric and gastroesophageal junction cancer endoscopic biopsies: is membrane expression in five cells enough?

Iglesias M [1,2], Rodrigo MT [1], Tagmouti G [1], Sabate J [3], Diaz L [1], Torner A [1], Salido M [1], Naranjo-Hans D [1], Gimeno J [1,2], Puiggros A [1], Espinet B [1], Lloveras B [1,2]

[1] Pathology Department. Hospital del Mar. Parc de Salut Mar. IMIM. Barcelona (Spain). [2] Autonomous University of Barcelona. [3] Oncology Department. Hospital del Mar. Parc de Salut Mar. Barcelona (Spain)

Background

HER2 overexpression/amplification should be determined in gastric (GC) or gastro esophageal junction cancer (GEJC) tributary for anti-HER2 treatment. In cases borderline/equivocal (2+) with immunohistochemistry (from weak to moderate intensity of membranous staining) an assessment of the amplification of the gene must be done by in situ hybridization (ISH) analysis. The immunohistochemistry cut-off varies between surgical specimen and endoscopic biopsy. The minimal threshold of cellular membrane expression in biopsy is five cells. Our aim is to analyze the correlation of this threshold with borderline expression with the amplification of the gene by ISH.

Design

Retrospective review of GC and GEJC cases in the Hospital del Mar of Barcelona between 2010 and 2016, with HER2 2+ studied by inmunohistochemistry (Ventana 4B5). The exact number or percentage of cells with expression of HER2 and the status of the gene using in situ hybridization were recorded and compared.

Results

We have reviewed 86 cases (63 biopsies and 23 surgical specimens). From the 63 endoscopic biopsies, we selected 46 cases HER2 2+ with a homogeneous intensity of HER2.

We found very weak staining (measured as weak staining saw at 20x) of HER2 in 9 cases (14.3%), weak staining, evaluated at 10x in 30 cases (47.6%), and moderate intensity in 7 cases (11.1%). Figure 1.

In terms of the number of cells and amplification, 2 cases with very weak expression depicted between 5 and 10% stained cells and were non-amplified by ISH and 7 cases had more than 10% positive cells and one of them were amplified. Fourteen cases with weak positivity presented ≥10% stained cells and 12 of them were non amplified, 5 cases with ≥5- <10% stained cells were non amplified and among 11 cases with <5% one case was amplified. All 7 moderately stained cases presented staining in ≥10% neoplastic cells and 3 of them were amplified. Figure 2 and 3.

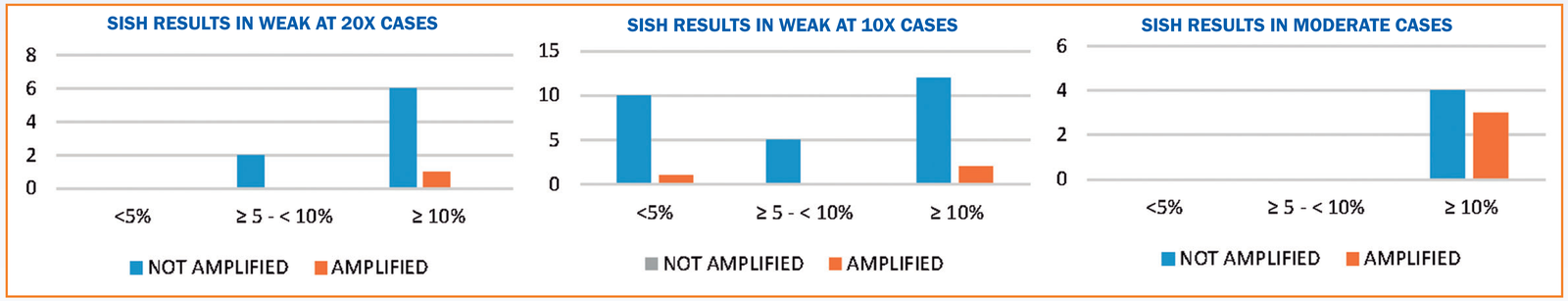

Figure 2. Distribution of Equivocal HER2 cases depending on the intensity of the membranous staining, the percentage of stained cells and the SISH results

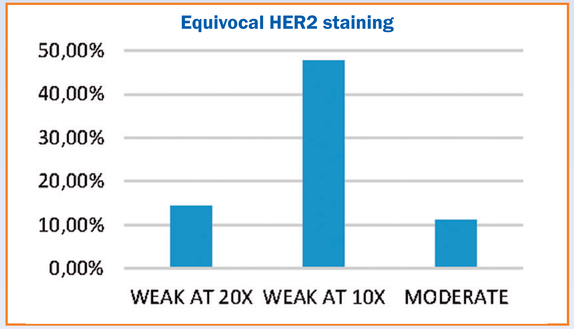

Figure 1. Percentage of cases depending on the intensity of the membranous staining

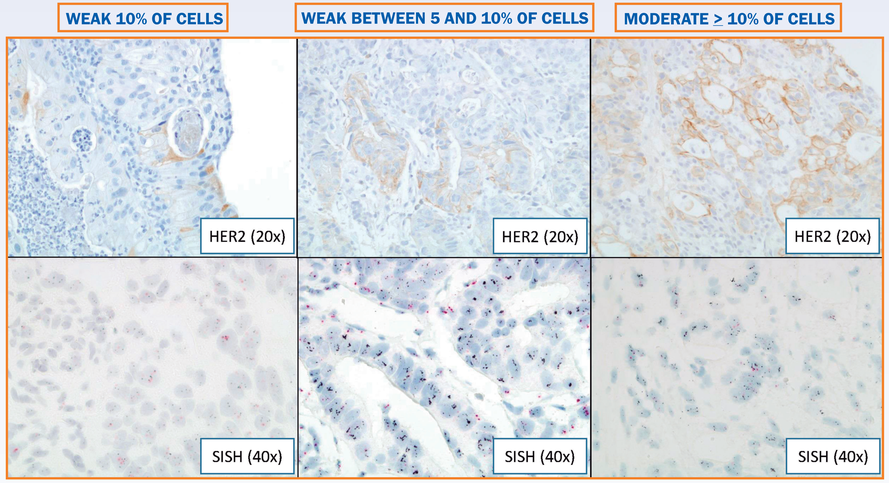

Figure 3. Examples of cases showing intensity of expression of amplified cases.

Conclusion

We have proved that the minimal threshold criteria used nowadays in biopsies, for HER2 testing, detected some amplified cases by ISH, even when there are only very few positive cells with weak membrane expression. The real impact of this finding regarding response to therapy deserves further analysis.

Bibliography

- Bang YJ et al. Trastuzumab in combination with chemotherapy versus chemotherapy alone for treatment of HER2-positive advanced gastric or gastro-oesophageal junction cancer (ToGA): a phase 3, open-label, randomised controlled trial. Lancet. 2010.
- Fernando López-Rios F et al. HER2 evaluation in gastric carcinoma: A consensus study by the Spanish Society of Pathology (SEAP) and the Spanish Society of Medical Oncology (SEOM). Rev Esp Patol. 2011.
- Rüschoff J et al. HER2 testing in gastric cancer: a practical approach. Mod Pathol. 2012.
- Bartley AN et al. HER2 Testing in Gastroesophageal Adenocarcinoma. Arch Pathol Lab Med. 2016..

Hospital del Mar

Parc de Salut MAR Barcelona

Ciliary Ultrastructural Features in a Cyclin O-Deficient Murine Model of the Reduced Generation of Multiple Motile Cilia Syndrome

Josep Lloreta-Trull[1,2,3], Mercedes Simon-Grimaldos[1], Marta Garrido[3], Silvia Hernández-Llodrà[2], Nuria Juanpere[1,2,3], Gabriel Gil-Gomez[3]

Hospital del Mar-Parc de Salut Mar[1], Universitat Pompeu Fabra[2], Hospital del Mar Research Institute[3], Barcelona, Spain

Background

The field of ciliary pathology has advanced exponentially with the use of molecular techniques, both for studying the genetic abnormalities related to ciliary motility and the molecular biology of ciliary biogenesis. Thus, nowadays electron microscopy (EM) is an excellent screening tool in ciliary dyskinesia but it is only a first step to indicate specific genetic tests that will result in the precise identification of the primary molecular defect. On the other hand, regarding ciliary biogenesis it is increasingly acknowledged that can be the source of many diseases that can relate to ciliary insufficiency without any abnormality in the axonemal structure. Two different pathways for ciliary biogenesis are currently accepted. The most frequent involves dividing cells in which there is a symmetric division of the centrioles to provide for an adequate mitotic organization and a homogeneous distribution in the daughter cells. This process is related to a centriole-forming structure called centrosome. On the other hand, ciliated cells such as those of the respiratory tract and the Fallopian tube or the ependymal cells are generated through a massive asymmetric process in which the mother centriole is not involved and that relies on the active division of the daughter centriole. In this process, the centrosome still has a role but a new yet still incompletely characterized organelle, the so-called deuterosome, has a major role as the center of the centriolar division process.

Recently, Cyclin O (CCNO) mutations were identified in a subset of Primary Ciliary Dyskinesia (PCD) patients affected by recurrent upper and lower airway infections, bronchiectasis, hydrocephalus (~10%), and reduced fertility. This PCD subset has been termed Reduced Generation of Multiple Motile Cilia (RGMC) and is also caused by mutations in the MCIDAS gene that is adjacent to CCNO on chromosome 5q. There are few reports on this syndrome, some of them based on animal models. Our laboratory has developed a constitutive loss-of-function mouse model with complete CCNO deficiency. There are very few data on the electron microscopic changes in cases of RGMC or on its murine counterparts. The aim of the present study has been to characterize the ultrastructural features of cilia and related structures in our CCNO deficiency murine model.

Design

This is a descriptive study of fine structural changes in two experimental groups, consisting respectively of three wild-type and three CCNO deficient mice. Transmission electron microscopy was performed on perfusion-fixed samples of brain periventricular ependymal cells, uterine tubal epithelium and tracheal mucosa. Uranyl acetate and lead citrate stained thin sections were examined in a Phillips-FEI CM100 electron microscope. The Ethics Guidelines for Laboratory Animal Research from the PSMAR Consortium (Parc de Salut Mar - Hospital del Mar Research Institute) were strictly followed.

Results

The most striking ultrastructural findings were detected in the ependymal and respiratory tract cilia. In the respiratory tract, compared to their normal counterparts (**Figure 1**), there was a marked reduction in the number of cilia in ciliated cells in the CCNO$^{-/-}$ mice (**Figure 2**). This could be recognized not only because there were cells with scanty ciliary structures (**Figure 2a**) but also because it was obvious that cells with much longer microvilli than their neighbors were actually ciliated cells without cilia (**Figure 2b**). Based on this finding, it could be stated that there was also a reduced number of potentially ciliated cells. On occasion, intraepithelial microcystic spaces were found in the respiratory epithelium of the defective mice (**Figure 2c**). In addition to a marked reduction in the number of cilia compared to controls, the most remarkable finding was the presence of severe defects in basal body formation (**Figure 2e through 3e**), with disassembled microtubular precursors that resulted in a meandering, spread-out or annular shape (**Figures 3e and e'**). In the vicinity of these abnormal basal bodies poorly defined deuterosomes were identified (**Figure 4**). The axial symmetry of cilia was not significantly lost, as evidenced by drawing lines through the center of the ciliary axoneme aligned with the central pair of tubules (**Figure 2d**). In spite of all these abnormalities, the few successful cilia that could be found had normal axonemes, without significant abnormalities of the doublets, dynein arms or nexin links. Radial spokes seemed to be partially lost in some of the cilia, although this could be a sampling or artifactual problem. The changes were particularly obvious in the respiratory epithelium but also evident in the ependymal cells (**Figure 5**).

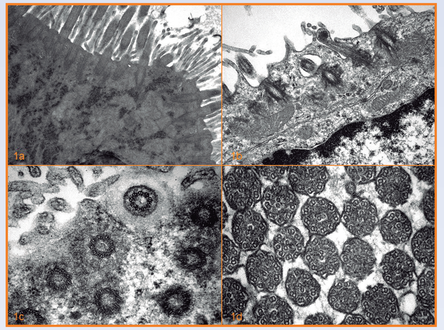

Figure 1. Respiratory epithelium in normal (CCNO$^{+/+}$) mice. **1a**/ Abundant cilia with normal basal bodies and long, slender adjacent microvilli. **1b**/ Budding cilia in a regenerating cell. **1c**/ Transverse section through basal bodies showing characteristic microtubular triplets. **1d**/ Normal axonemes in this image show a slight axial misalignment.

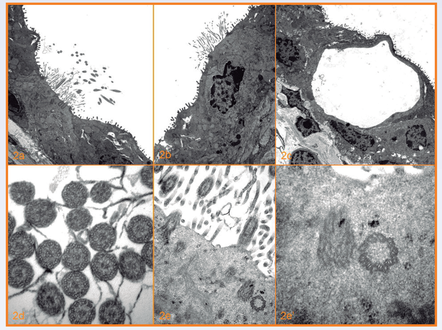

Figure 2. Respiratory epithelium in defective (CCNO$^{-/-}$) mice. **2a**/ Ciliated cell with reduced number of cilia. **2b**/ Ciliated cell with complete lack of cilia. It can be assumed to be a ciliated cell because of the much longer microvilli compared to the neighbor, non-ciliated cells. **2c**/ Microcyst-like spaces were occasionally found in the respiratory epithelium. **2d**/ In the existing cilia, the axoneme was normal and the alignment was preserved. **2e**/ Basal body defects were heterogeneously distributed. This cell has one normal basal body and the remaining ones are poorly formed. **2e'**/ Close-up view of a well-developed basal body and a poorly defined, irregular one.

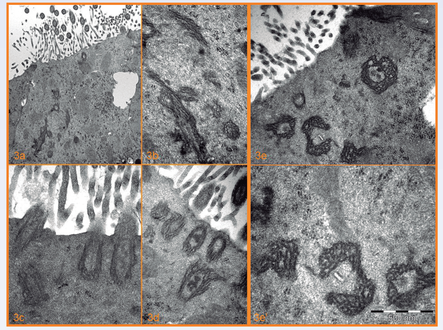

Figure 3. **Range of basal body formation abnormalities** observed in this experimental model. **3a**/ Cluster of incomplete basal bodies probably concentrated around a deuterosome. **3b**/ Close-up view of the same cluster. **3c**/ Mild defects in the definitive apical basal bodies are evident. **3d**/ Moderate to severe defects in basal bodies in this cell. **3e and e'**/ Meandering precursors of basal bodies of different shapes.

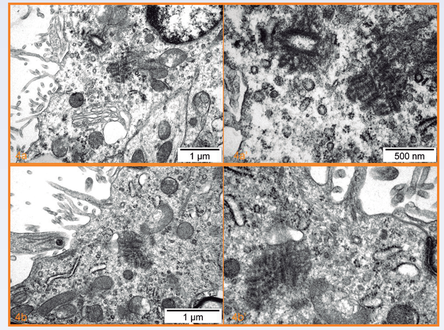

Figure 4. Budding centrioles around a deuterosome are seen in two different cells: **4a and a'** and **4b and b'.**

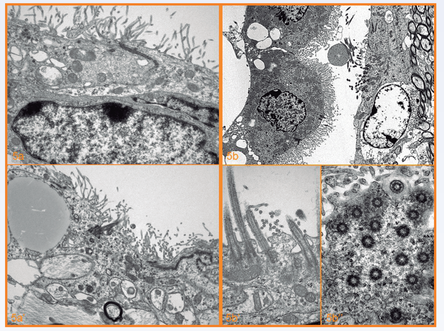

Figure 5. Ependymal cells of CCNO deficient (**5a and 5a'**) and wild type mice (**5b, 5b' and 5b''**). The extreme reduction in cilia in the ependymal cells was associated to the development of a hydrocephalus. **5b**/ Confronting ependymal (right) and choroidal plexus (left) cells.

Conclusion

The constitutive CCNO-deficient mouse model is characterized by abnormalities related to early ciliogenesis, basal body formation and ciliary polarity. This may explain the more severe abnormalities, mostly hydrocephalus, that affect these mice and to a lesser degree patients with CCNO deficiency. This animal model can be useful in the investigation of the increasingly complex field of ciliary dyskinesia.

References

- Funk MC, Bera AN, Menchen T et al. Cyclin O (Ccno) functions during deuterosome-mediated centriole amplification of multiciliated cells. EMBO J. 2015.
- Jord AA, Lemaître AI and Delgehyr N et al. Centriole amplification by mother and daughter centrioles differs in multiciliated cells. Nature 2014; 516:104-7.
- Nuñez-Olle M, Jung C, Terré B, et al. Constitutive Cyclin O deficiency results in penetrant hydrocephalus, impaired growth and infertility. Oncotarget 2017: 8:99261-73.
- Wallmeier J, Al-Mutairi DA, Chen CT et al. Mutations in CCNO result in congenital mucociliary clearance disorder with reduced generation of multiple motile cilia. Nat Genet 2014; 46(6):646-51.
- Yan X, Zhao H, Zhu X. Production of basal bodies in bulk for dense multicilia formation. F1000Research 2016; 5:1533-9..

Hospital del Mar

Parc de Salut MAR Barcelona

ETS Genes (*ERG, ETV1, ETV4* and *ETV5*) overexpression and *PTEN* Loss in Prostate Cancer

Laura Segalés[a], Nuria Juanpere[a,b], Silvia de Muga[a], Marta Lorenzo[b], Lluis Fumadó[c,d], Lluis Cecchinni[c,d], Belén Lloveras[b,d], Josep Lloreta[a,b] and Silvia Hernández-Llodrà[a]

Department of Health and Experimental Sciences, Universitat Pompeu Fabra[a], Department of Pathology[b] and Department of Urology[c], Hospital del Mar-Parc de Salut Mar-IMIM, and Autonomous University of Barcelona[d], Barcelona, Spain.

Corresponding author: laura.segales01@estudiant.upf.edu

Introduction

The molecular taxonomy of primary Prostate Cancer (PrCa) was reported by the Cancer Genome Atlas (TCGA) research network in 2015, and seven PrCa subtypes defined by *ETS* fusions or mutations in driver genes were established. *ERG* is an *ETS*-family member overexpressed in most of the *TMPRSS2-ERG* rearranged prostate tumors and *PTEN* loss is often a concomitant event. However, there is a remarkable molecular diversity among the ETS-fused prostate tumors. Other *ETS* members, such as *ETV1, ETV4,* and *ETV5*, are also overexpressed in PrCa, but with a lower frequency. The relationship between this overexpression, the aberrant mechanisms that induce it, and the consequences on the clinical-pathological features of the respective prostate tumors is incompletely understood.

Objectives

The aim of the present study has been to investigate the effect of the rearrangements between *TMPRSS2* and several *ETS* genes on the overexpression of the latter, and to assess the relationship of this overexpression and *PTEN* loss with the main clinical-pathological parameters of PrCa.

Material and methods

Tumor Samples and Patients.-

A hundred and six frozen prostate tumors and 3 benign prostate tissue samples were selected retrospectively from the files of the Parc de Salut MAR Biobank (MARBiobanc), Barcelona, Spain. According to the new Grade Group (GG) proposal by the WHO-ISUP 2016, samples were classified as: GG1 (n = 27), GG2 (n = 33), GG3 (n = 21), GG4 (n = 14) and GG5 (n = 11).

RNA Extraction and Retrotranscription.-

Total RNA was extracted from all tumor samples and the 3 benign tissues. RNA purity and quality were assessed with the NanoDrop® (NanoDrop Technologies, USA) and the Agilent 2100 Bioanalyzer (Agilent, USA). cDNA was synthesized using 1µg of total RNA and Superscript IV Kit (Invitrogen, Life Technologies Corporation, CA, USA).

ERG, ETV1, ETV4, ETV5 and *PTEN* expression analysis by RT-qPCR.-

RT-qPCR analysis was done from cDNA and using the TaqMan® Gene Expression Assays (Thermo Fisher Scientific MA, USA) shown in Table 1. Samples were run in triplicate and *GADPH* was used as internal control. *ETS* genes overexpression was considered for values of $2^{(-\Delta\Delta Ct)} \geq 2.2$ times the average levels of the non-tumor controls, while *PTEN* loss of expression cut-off was $2^{(-\Delta\Delta Ct)} \leq 0.35$.

TMPRSS2-ERG, TMPRSS2-ETV1, TMPRSS2-ETV4, TMPRSS2-ETV5 and *ERG* control analysis by RT-PCR.-

The *TMPRSS2-ETS* rearrangements expression was analyzed by RT-PCR. A region located between exons 4 and 5 of *ERG* was used as control and it was successfully amplified in all samples. Primers are shown in Table 2. For the detection of the rearrangements among *ETS* genes and *TMPRSS2*, a semi-quantitative assessment of the expression was carried out by comparing the intensity of the rearrangement *PCR* product and the *ERG* control. Two categories, positive and negative cases, were established.

PCR product purification and Sanger direct sequencing.-

The *TMPRSS2-ETS* rearrangement PCR products were purified. Sanger sequencing reactions were done with Big Dye Terminator Kit v.3.1 (Thermo Fisher Scientific MA, USA) and the same primers used in the PCR amplifications.

Table 1. Applied Biosystems Taqman ® RT-qPCR assay identification number.

Genes/Fusion variants amplified	Assay Identification number
ERG	*Hs01554629_m1*
ETV1	*Hs00951951_m1*
ETV4	*Hs00383361_g1*
ETV5	*Hs00927557_m1*
PTEN	*Hs02621230_s1*
GAPDH	*4310884E – NM_002046.3*

Table 2. Primers used for *ETS* gene rearrangements RT-PCR analysis.

Genes/Fusion variants amplified	Forward primer	Reverse primer
TMPRSS2-ERG	GCGCCGCCTGGAGCGCGGCA	GGCGGGAAGATGGTGGGCAG
TMPRSS2-ETV1	GCGCCGCCTGGAGCGCGGCA	CACTGCATCATGCATCTCCA
TMPRSS2-ETV4	TTTCTCCCCGCTTCTCGCA	TCAGGTACCAGACAGTGATG
TMPRSS2-ETV5a	GCGCCGCCTGGAGCGCGGCA	TCAGCAAGTCCCTTTTATGG
TMPRSS2-ETV5b	ACCACCAGCTATTGGACCTT	TCAGCAAGTCCCTTTTATGG
ERG	GGAAGCCTTATCAGTTGTGA	GGCGGGAAGATGGTGGGCAG

Conclusions

- *ERG* is the most frequently overexpressed *ETS* gene, followed by *ETV1*, *ETV4*, and *ETV5*.
- Most of the *ETS* genes are overexpressed as a single event.
- *ETS* overexpression plus *PTEN* loss is a very frequent event in PrCa, and *PTEN* loss is associated with single *ETS* overexpression.
- Single *ETS* gene overexpression shows a trend to be associated with low GG tumors.
- There is a non-significant trend for cases overexpressing multiple *ETS* genes to be GG4 PrCa.
- In the *ETS*-overexpressing cases, most high GG tumors had *PTEN* loss.
- There is a strong correlation between *ERG* overexpression and *TMPRSS2-ERG* rearrangement.
- *ETV4* overexpression seems to be associated with *TMPRSS2-ETV4*, whereas correlation has not been noted for *ETV1* and *ETV5* overexpression with their rearrangement with *TMPRSS2*.

Results

Overexpression of *ETS* genes and *PTEN* loss in Prostate Cancer.-

Seventy-four prostate tumors (69.8%) presented overexpression of one or more than one *ETS* genes [Figure 1A]. *ERG* was the most frequently overexpressed gene (55.6%), followed by *ETV1* (18.8%), *ETV4* (7.5%), and *ETV5* (5.6%) [Figure 1B]. *ETS* genes were usually overexpressed as a single event. Sixty-two tumors (58.5%) presented overexpression of a single *ETS* gene, while there were 12 (11.3%) with high expression levels of multiple *ETS* genes [Figure 2A]. In addition, *ERG* overexpression was statistically associated with basal levels of the other *ETS* genes (*Pearson* X^2, *P=0.04*) [Figure 2B].

PTEN expression loss was found in 44 (41.5%) of our PrCa series [Figure 3A]. Combined *ETS* gene overexpression and *PTEN* loss was detected in 37 tumors (34.9%). *ETS* gene overexpression was seen in 84.1% of the tumors with *PTEN* loss, while only 7 cases (15.9%) presented with *PTEN* loss alone. There was a correlation between single *ETS* overexpression and *PTEN* loss (*Pearson* X^2, *P=0.0024*) [Figure 3B].

Overexpression of *ETS* genes, *PTEN* loss and Grade Group tumor classification.-

Single *ETS* overexpression was more frequent in GG1-3 PrCa (*Not Significant, N.S.*), while overexpression of multiple *ETS* genes was more frequently found in GG4 tumors (N.S.), and basal expression levels of all *ETS* genes was more prevalent in GG5 PrCa (*N.S.*) [Figure 4]. Only 18.2% of GG5 tumors showed single *ERG* overexpression (*N.S.*).

PTEN loss was less frequently detected in low GG PrCa (N.S.) [Figure 5A]. Taking into account only the *ETS*-overexpressing tumors, 80% of GG5 PrCa had *PTEN* loss (*N.S.*) [Figure 5B].

ETS gene rearrangements with *TMPRSS2*.-

Chromosomal fusions affecting *TMPRSS2* and one of the *ETS* genes were detected in 66 tumors (62.3%). Sixty-three of the 66 fusion-positive prostate tumors (95.5%) harbored a single rearrangement between *TMPRSS2* and one of the *ETS* genes, while only 3 rearranged PrCa (4.5%) harbored multiple *TMPRSS2-ETS* fusions [Figure 6].

Overexpression of *ETS* genes and respective *TMPRSS2* fusions.-

ERG overexpression and the *TMPRSS2-ERG* rearrangement showed a very strong correlation. Only four of the 59 *ERG*-overexpressing PrCa (6.8%) were not rearranged. By constrast, only 1 of the 20 (5%) *ETV1*-overexpressing tumors was positive for *TMPRSS2-ETV1*. The *TMPRSS2-ETV4* rearrangement was detected in 6 of the 8 tumors (75%) that overexpressed ETV4 and the *TMPRSS2-ETV5* rearrangement was not identified in any the 6 tumors that overexpressed *ETV5*.

Figure 1. Prevalence of *ETS* gene overexpression [A and B].

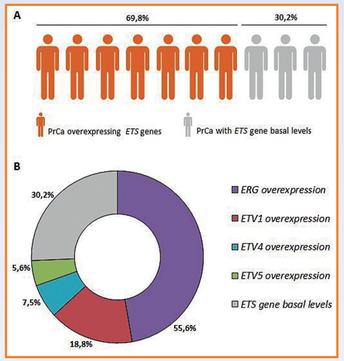

Figure 2. Prevalence of single and multiple *ETS* gene overexpression [A]. Relationship between *ERG* and other *ETS* gene overexpression [B].

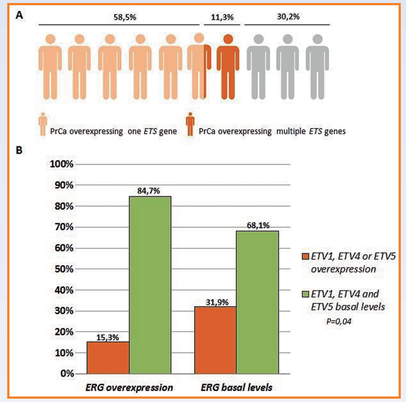

Figure 3. Prevalence of *PTEN* expression loss [A]. Relationship between *PTEN* loss and single, multiple or no *ETS* gene overexpression [B].

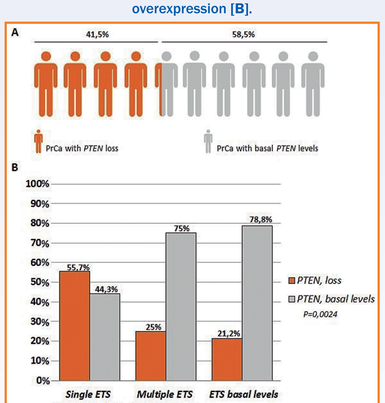

Figure 4. Single, multiple or no *ETS* gene overexpression according to the Grade Group tumor classification.

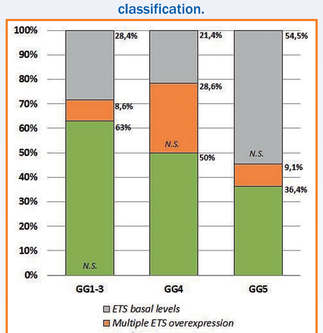

Figure 5. *PTEN* loss and Grade Group tumor classification [A]. *PTEN* loss and Grade Group tumor classification in the *ETS*-overexpressing tumors [B].

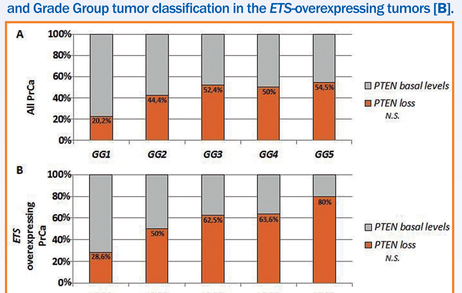

Figure 6. Distribution of the *ETS* gene rearrangements with *TMPRSS2*.

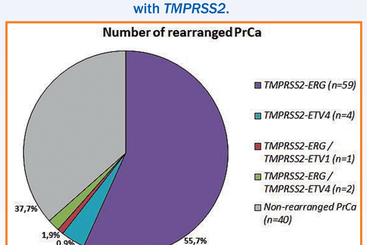

References

- Oikawa T, Yamada T. Molecular biology of the Ets family of transcription factors. *Gene*, 2002; 11-34.
- Tomlins S, Rhodes DR, Perner S, et al. Recurrent fusion of TMPRSS2 and ETS transcription factor genes in prostate cancer. *Science*, 2005; 644-648.
- Kumar-Sinha C, Tomlins SA, Chinnaiyan AM. Recurrent Gene Fusions in Prostate Cancer. *Nat Rev Cancer*, 2008; 724-732.
- Clark J, Cooper C. ETS gene fusions and prostate cancer. *Am J Transl Res*, 2009;341-351.
- Shaikhibrahim Z, Braun M, Nikolov P, et al. Rearrangement of the ETS genes ETV-1, ETV-4, ETV-5, and ELK-4 is a clonal event during prostate cancer progression. *Hum Pathol*, 2012; 1910-1916.
- Barbieri CE, Tomlins S. The prostate cancer genome: Perspectives and potential. *Urol Oncol Semin Orig Investig*, 2014; 15-53.
- Abeshouse A, Ahn J, Akbani R, et al. The Molecular Taxonomy of Primary Prostate Cancer. *Cell*, 2015; 1011-1025.
- Hernández S, Font-Tello A, Juanpere N, et al. Concurrent TMPRSS2-ERG and SLC45A3-ERG rearrangements plus PTEN loss are not found in low grade prostate cancer and define an aggressive tumor subset. Prostate, 2016; 854-865.

Support Grants:
(FIS/ Carlos III/ FEDER/ PI15/00452, Spanish Ministry of Health).

Hospital del Mar

Parc de Salut MAR Barcelona

Analysis of *MET* Exon 14 Skipping Mutations and *MET* Gene Amplifications in Non Small-Cell Lung Cancer Patients

Marta Salido[1,2], Sergi Clavé[1,2], Alba Dalmases[1,2], Lara Pijuan[1], Raquel Longaron[1], Marta Lorenzo[1,2], Álvaro Taus[4], Erica Torres[1], Pedro Rocha[4], Blanca Espinet[1,2], Beatriz Bellosillo[1,2], Edurne Arriola[2,4]

1. Servei de Patologia, Hospital del Mar, Barcelona. 2. Programa de Recerca en Càncer, Institut Hospital del Mar d'Investigacions Mèdiques, Barcelona. 3. Servei d'Oncologia, Hospital del Mar, Barcelona.

Disclosure: The authors certify no conflict of interest. Contact: msalido@hospitaldelmar.cat

Background

- In lung cancer, the landscape of mesenchymal–epithelial transition factor (*MET*) oncogenic alterations consists on mutations leading to the skipping of exon 14 (*MET*ex14) or *MET* amplification.
- *MET*ex14 mutations and primary *MET* amplification are likely to represent an actionable driver oncogenic target in a small subgroup (2-5%) of NSCLC patients, predominantly adenocarcinomas (ADC).
- Correlation among *MET*ex14 mutations and *MET* amplification remain unclear.
- Our aim was to investigate the coexistence of *MET*ex14 skipping and *MET* copy number alterations (CNAs).

Design

- A total of 222 paraffin-embedded NSCLC samples selected from 2013 to 2016 were included.
- Patient's characteristics were: median age 64 year-old, 72% were males, 84% were current or former smoker, 54% were diagnosed in advanced stage and 85% were adenocarcinomas.
- *MET*ex14 and flanking intron mutations were studied by PCR-direct sequencing using DNA extracted from paraffin blocks.
- CNAs were analyzed by fluorescence in situ hybridization (FISH) with the MET / CEP7 probe (Abbott Molecular). Amplifications were defined as mean gene by mean centromere ratio ≥1.8, and high amplified cases were defined by ratio ≥5.0. (Figure 1)
- When possible, reverse transcriptase PCR (RT-PCR) was performed to validate mutations leading to exon 14 skipping.
- We collected clinical-pathological data together with *EGFR* and *KRAS* mutational status and *ALK*, *ROS1* and *RET* rearrangements.

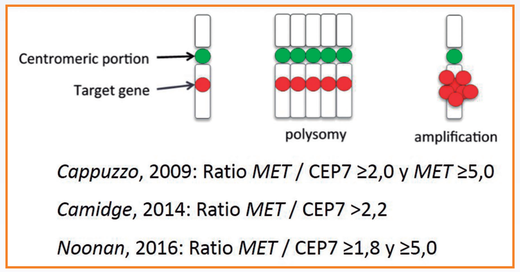

Figure 1. FISH criteria to determine the *MET* amplification. The ratio MET/CEP7 allow us to rule out the possibility of polyploidy.

Results

- *MET* alterations were found in 24 patients (10.8%): 12 mutated and 13 amplified cases (Table 1, Figure 2 and 3).
- Five of the 12 *MET* mutations (5/222; 2.2%) were confirmed to lead exon 14 skipping.
- Regarding concurrent alterations, in one of these cases we identified also *MET* amplification and two cases had *KRAS* mutation.
- Regarding clinical data among patients with *MET* alterations (n=24), 23 were men (96%), with a mean age of 62 years-old (range: 40-91), 16 were active smokers and 17 were diagnosed in the advanced stage (70.8%).

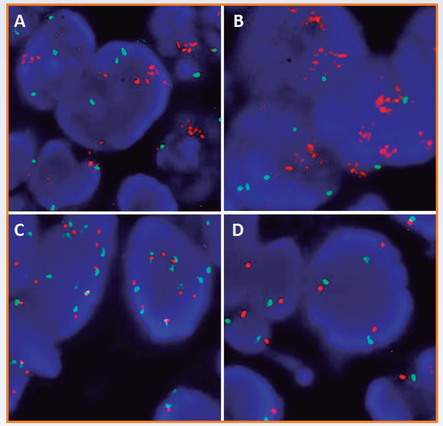

Figure 2. Representative FISH images of *MET* copy number alterations. *MET* is labeled in spec. Orange and CEP7 in spec. Green (Abbott Molecular). (A) MET amplification with a ratio *MET*/CEP7 of 2.2. (B) *MET* cluster amplification with a ratio *MET*/CEP7 >5. (C) Case with a high polysomy of chromosome 7, ratio *MET*/CEP of 1.2. (D) Case with a low polysomy 7.

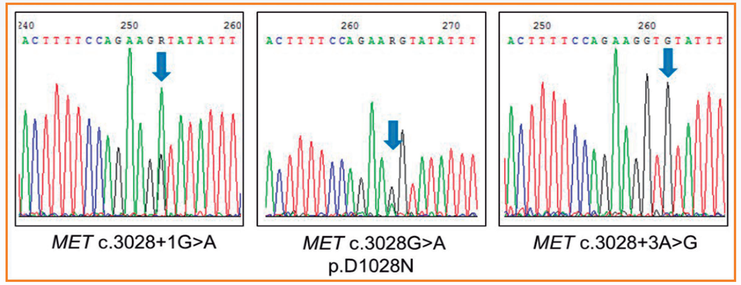

Figure 3. Representative images of METex14 mutations in NSCLC. The nucleotide changes in the chromatograms are indicated by arrows.

Table 1. *MET* gene alterations and variants found in lung non-small cell carcinomes (NSCLC).

ID	Gender	Age	Smoker	Histology	TNM	Stage	MET Mutation	MET status	MET FISH	MET/CEP7 RATIO	Concomitant Alterations
T1	MALE	78	Former	ADC	T2aN1M0	II	c.3028+1G>A	SKIPPING	HIGH CNG	1,68	KRAS p.G12A
T2	MALE	53	Current	NSCLC NOS	T2bN2M0	III	p.R988C	PATHOGENIC	POLYSOMY	0,49	WT
T3	MALE	67	Current	ADC	TxN2M1a	IV	p.T995I	UNKNOWN	NON AMPLIFIED	1	WT
T4	MALE	66	Former	ADC	T1bN3M1b	IV	p.D999N	UNKNOWN	POLYSOMY	0,9	WT
T5	MALE	52	Current	ADC	T2aN2M0	II	p.T1010I	PATHOGENIC	POLYSOMY	1,12	WT
T6	MALE	60	Current	ADC	T4N1M1b	IV	p.S1018C	PATHOGENIC	POLYSOMY	1,14	WT
T7	MALE	91	Former	ADC	T3N2M0	III	c.3028+1G>A	SKIPPING	NON AMPLIFIED	1,05	WT
T8	MALE	78	Never	ADC	T4N0M0	I	c.3028+1G>A	SKIPPING	NON AMPLIFIED	1,02	WT
T9	MALE	80	Former	ADC	T2aN1	I	c.3028+2T>A	SKIPPING	AMPLIFIED	1,81	WT
T10	MALE	76	Never	ADC	T2aN0M1a	IV	c.3028+3A>G	UNKNOWN	POLSOMY	0,47	WT
T11	MALE	40	Current	ADC	T4N3M1b	IV	c.3028+5T>G	UNKNOWN	-	-	EGFR DEL EX19
T12	FEMALE	53	Current	ADC	T1aN0M0	I	p.D1028N	SKIPPING	POLYSOMY	0,9	KRAS p.G12C
T13	MALE	60	Former	NET	T3N0M0	III	WT	-	AMPLIFIED	1,93	WT
T14	MALE	43	Current	ADC	TxN2M1a	IV	WT	-	AMPLIFIED	1,86	ALK+
T15	MALE	40	Current	ADC	T3N3M0	III	WT	-	AMPLIFIED	2,69	WT
T16	MALE	72	Former	ADC	T4N1M0	III	WT	-	AMPLIFIED	2,22	EGFR p.V774M
T17	MALE	53	Current	ADC	T2N2M0	III	WT	-	AMPLIFIED	2,92	WT
T18	MALE	56	Former	ADC	T2N0M0	I	WT	-	AMPLIFIED	2,82	WT
T19	MALE	64	Current	CA ADC	T1bN0M0	I	WT	-	AMPLIFIED	2,4	WT
T20	MALE	73	Former	NSCLC NOS	TxN3M0	III	WT	-	AMPLIFIED	2,38	WT
T21	MALE	46	Current	ADC	T1bN3M1b	IV	WT	-	AMPLIFIED	5,65	WT
T22	MALE	71	Current	ADC	T1bN3M1b	IV	WT	-	AMPLIFIED	6,1	WT
T23	MALE	71	Former	ADC	T2bN3M1b	IV	WT	-	AMPLIFIED	8,6	WT
T24	MALE	55	Current	ADC	T3N3M1b	IV	WT	-	AMPLIFIED	3,8	WT

AD:Adenocarcinoma; CA: carcinoma; NSCLC NOS: non-small cell lung carcinoma not otherwise specified; NET: Neuroendocrine Tumor
WT: wild-type

Conclusions

- *MET*ex14 skipping mutations define a small subgroup of patients with NSCLC.
- Rarely, *MET* gene amplification might coexist with *MET* mutation.
- Both, *MET*ex14 skipping mutations and *MET* CNAs represent a new therapeutic target for patients with NSCLC and should be incorporated to the diagnostic protocols of these patients.

ERG, Prostein and PTEN Expression and their Relationship with Epithelial-Mesenchymal Transition, Stemness and Apoptosis Molecules in Prostate Cancer

Nuria Juanpere MD[1,3], Silvia Hernández-Llodrà PhD[3], Marta Lorenzo[1], Silvia de Muga PhD[1,3], Joan Gil[3], Raquel Albero MD[1], Ivonne Vázquez MD[1], Lluís Fumadó MD,PhD[2,4], Lluís Cecchini MD,PhD[2,4], Belén Lloveras MD,PhD[1,4] and Josep Lloreta MD,PhD[1,3]

Department of Pathology[1] and Urology[2], Hospital del Mar-Parc de Salut Mar-IMIM; Universitat Pompeu Fabra[3] and Autonomous University of Barcelona[4], Barcelona, Spain

Background

TMPRSS2-ERG rearrangement is the most common genetic alteration in prostate cancer (PrCa). It has been reported as an early event in prostate carcinogenesis but its role in PrCa development is still controversial. *ERG* fusion with *SLC45A3* (Prostein), a gene involved in prostatic differentiation, is the second most common rearrangement. *PTEN* loss is a crucial step in PrCa pathogenesis and has been associated with high grade tumours. In an ERG+ subset of prostate cancer (PrCa), we reported that combined ERG expression, Prostein loss and PTEN loss ("triple hit" or 3-hit) is associated with high grade and stage PrCa and with shorter PSA progression-free survival, while ERG expression alone is related to lower Grade group tumors.

E-cadherin is an adhesion molecule related to cell differentiation. β-Catenin is a submembrane protein involved in cell adhesion and signal transduction and forms a complex with E-cadherin. Loss of E-cadherin and β-Catenin membrane expression (and translocation to the nucleus for the latter) are markers of epithelial-mesenchymal transition (EMT), a process through which epithelial cells acquire motility, invasive properties and metastatic potential. CD44, an adhesion molecule expressed in prostate basal cells, has been reported in a subpopulation of prostate stem cells with tumor-initiating and metastatic potential. Bcl-2 protein has anti-apoptotic effects and has been involved in PrCa chemoresistance.

The aim of the present study has been to investigate by means of immunohistochemistry the relationship of ERG, Prostein and PTEN expression with E-cadherin, β-Catenin, CD44 and Bcl-2, as markers of EMT, stemness and apoptosis regulation, respectively, in a series of PrCa.

Design

A TMA series with 220 radical prostatectomies (with a mean of three cores per case), selected retrospectively from the files of the Parc de Salut MAR Biobank (MARBiobanc, Barcelona, Spain), was stained with antibodies against ERG (primary rabbit anti-ERG monoclonal antibody (Ab) (clone EPR3864, Epitomics, Burlingame, CA, USA)), Prostein (mouse monoclonal Ab (clone 10E3, Dako)), PTEN (mouse monoclonal Ab (clone 6H2.1, Dako)), E-cadherin (mouse monoclonal Ab (clone 36, Ventana, Roche)), β-Catenin (mouse Ab (clone 14, Ventana, Roche)), Bcl-2 (CONFIRM anti-bcl-2 mouse monoclonal Ab (clone 124, Ventana, Roche)) and CD44 (rabbit monoclonal Ab (clone SP37, Ventana, Roche)), with the Dako Envision+ System-HRP (Dako, Glostrup, Denmark). The results were assessed by a team led by two pathologists.

ERG was considered positive (as a result of its rearrangement) when nuclear expression in PrCa cells was found. Endothelial cells were used as internal positive control.

Prostein loss (as a result of its rearrangement as well) was assessed as follows: score 0 (absence or marked loss of cytoplasmic expression in PrCa cells when compared to benign prostate glands), score 1 (partial loss of cytoplasmic expression) and score 2 (intense, homogeneous cytoplasmic expression). **PTEN** loss was also evaluated with a three-tiered classification: score 0 (complete loss of nuclear and cytoplasmic expression in PrCa cells when compared to benign prostate glands), score 1 (partial loss of nuclear and cytoplasmic expression) and score 2 (preserved nuclear and cytoplasmic expression). We considered that there was **E-cadherin** and **β-Catenin** loss when they were completely negative or when there was a partial loss of membrane expression compared to benign prostate glands. **Bcl-2** loss was considered when there was absent or weak cytoplasmic expression when compared to benign glands. **CD44** expression was assessed in the membrane of PrCa cells, using basal cells as internal positive control.

Results

From 98 ERG+ PrCa, Bcl-2 expression was found in 44 (44.7%) *versus (vs)* 31/108 ERG- cases (26.7%) (p= 0.015) (**Figure 1**). From 85 ERG- (wild type) PrCa, 58 were CD44+ (68.2%) *vs* 35/67 ERG+ PrCa (52.2%) (p= 0.044) (**Figure 2**). From 64 cases with Prostein loss, 29 (45.3%) were associated with E-cadherin loss in contrast with 19/136 Prostein wild type (*wt*) cases (13.6%) (p< 0.0001) (**Figure 3**). From 65 cases with Prostein loss, β-Catenin was lost in 25 (38.4%) *vs* 34/138 Prostein *wt* cases (24.6%) (p= 0.042) (**Figure 4**). From 73 PrCa with PTEN loss, 26 (35.6%) were associated to E-cadherin loss *vs* 22/127 PTEN *wt* cases (17.3%) (p= 0.0035) (**Figure 5**). Finally, from 21 cases with the 3-hit, 15 (71.4%) were associated to E-cadherin loss compared to 33/179 non-3-hit cases (13.4%) (p< 0.0001) (**Figure 6**). For a summary of the results see **Table 1**.

Table1: Summary of results.

	E-cadherin loss	Pearson	β-Catenin loss	Pearson	Bcl-2 +	Pearson	CD44 +	Pearson
ERG +	29.9% (29/97)	0.0580	27.7% (27/97)	0.6801	**44.7% (44/98)**	**0.0158**	52.1% (35/67)	**0.0445**
Prostein loss	**45.3% (29/64)**	**<0.0001**	**38.4% (25/65)**	**0.042**	34.7% (23/66)	0.749	54.5% (24/44)	0.283
PTEN loss	**35.6% (26/73)**	**0.0035**	**34.7% (26/75)**	0.189	37% (27/73)	0.899	56.1% (32/57)	0.3229
"3-hit"*	**71.4% (15/21)**	**<0.0001**	45.5% (10/22)	0.0758	27.3% (6/22)	0.569	40% (6/15)	0.0761

*"3-hit": Triple hit (ERG expression, Prostein loss and PTEN loss).

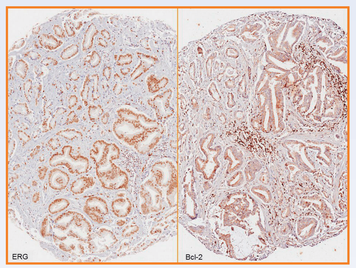

Figure 1. Grade group 3 prostate cancer with nuclear ERG expression (internal positive control in endothelial cells) and Bcl-2 cytoplasmic expression (lymphocytes as internal positive control).

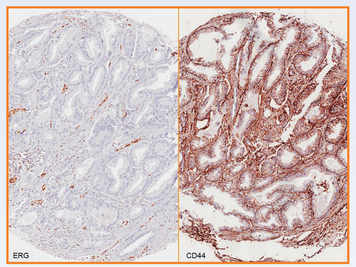

Figure 2. Grade group 1 prostate cancer (3+3= 6 Gleason score) without ERG expression (*ERG wt*) (internal positive control in endothelial cells) and with CD44 membrane expression.

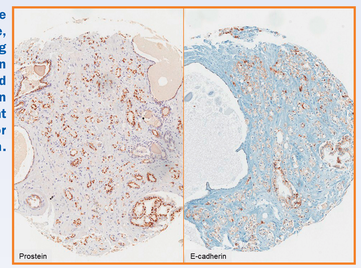

Figure 3. Grade group 5 prostate cancer (4+5= 9 Gleason score, with tertiary pattern 3) showing score 1 (partial loss) Prostein cytoplasmic expression and partial loss of E-cadherin membrane expression. Note that atrophic glands show weak or absent Prostein expression.

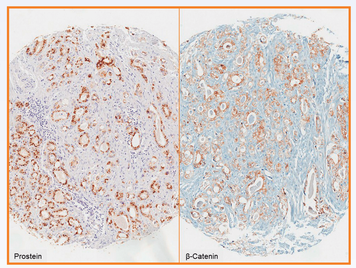

Figure 4. Grade group 3 prostate cancer with score 1 (partial loss) Prostein expression and partial loss of β-Catenin membrane expression.

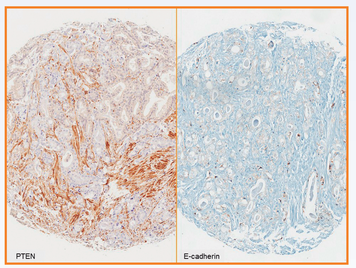

Figure 5. Grade group 3 prostate cancer with weak and focally absent nuclear and cytoplasmic PTEN expression and almost complete loss of E-cadherin membrane expression.

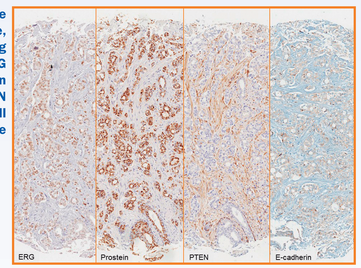

Figure 6. Grade group 4 prostate cancer (4+4= 8 Gleason score, with tertiary pattern 5) showing a triple hit phenotype (ERG nuclear expression, Prostein score 1 (partial loss) and PTEN score 0 (complete loss)) as well as weak E-cadherin membrane expression.

Conclusion

In our PrCa series, Bcl-2 is more commonly expressed in ERG expressing tumors and, on the other hand, CD44 expression is significantly related only to the ERG negative PrCa subset. Prostein loss, PTEN loss and the "triple hit" combination (ERG expression, Prostein loss and PTEN loss) are significantly associated with changes in adhesion molecules involved in epithelial-mesenchymal transition (E-cadherin and β-Catenin loss). These changes are probably related to the higher aggressiveness of this subset of tumors.

Supported by: FIS/Carlos III/FEDER/PI15/00452, Spanish Ministry of Health.

References

- Chen L, Mai W, Chen M et. al. Arenobufagin inhibits prostate cancer epithelial-mesenchymal transition and metastasis by down-regulating ?-catenin. Pharmacol Res. 2017; 123:130-142.
- Hernández-Llodrà S, Juanpere N, de Muga S et. al. ERG overexpression plus SLC45A3 (prostein) and PTEN expression loss: Strong association of the triple hit phenotype with an aggressive pathway of prostate cancer progression. Oncotarget. 2017 May 26. doi: 10.18632/oncotarget.18266. [Epub ahead of print].
- Hernández S, Font-Tello A, Juanpere N et. al. Concurrent TMPRSS2-ERG and SLC45A3-ERG rearrangements plus PTEN loss are not found in low grade prostate cancer and define an aggressive tumor subset. Prostate. 2016; 76:854–865.
- Font-Tello A, Juanpere N, de Muga S et. al. Association of ERG and TMPRSS2-ERG with grade, stage, and prognosis of prostate cancer is dependent on their expression levels. Prostate. 2015; doi:10.1002/pros.23004.
- Liu C, Kelnar K, Liu B et. al. Identification of miR-34a as a potent inhibitor of prostate cancer progenitor cells and metastasis by directly repressing CD44. Nat Med. 2011; 17(2): 211-215.
- Lotan TL, Gurel B, Sutcliffe S et al. PTEN protein loss by immunostaining: analytic validation and prognostic indicator for a high risk surgical cohort of prostate cancer patients. Clin Cancer Res. 2011; 17:6563–6573.
- Tomlins SA, Laxman B, Varambally S et. al. Role of the TMPRSS2-ERG gene fusion in prostate cancer. Neoplasia. 2008; 10:177–188.
- Whitaker HC, Girling J, Warren AY et al. Alterations in β-Catenin expression and localization in prostate cancer. Prostate. 2008; 68:1196-1205.

SPOP mRNA Downregulation Is Associated with TMPRSS2-ERG Fusion and PTEN Loss in Prostate Cancer

Silvia Hernández-Llodrà[a], Laura Segalés[a], Nuria Juanpere[a,b], Marta Lorenzo[b], Alba Font-Tello[a,e], Lluís Fumadó[c], Lluís Cecchinni[c,d] and Josep Lloreta[a,b]

Department of Health and Experimental Sciences, Universitat Pompeu Fabra[a] Department of Pathology[b] and Department of Urology[c], Hospital del Mar-Parc de Salut Mar-IMIM, and Autonomous University of Barcelona[d], Barcelona, Spain. Dana Farber Cancer Institute[e], Boston, USA

Introduction

The great majority of cases of prostate cancer (PrCa) harbor gene rearrangements in members of the *ETS* family. *TMPRSS2-ERG* has been reported as an early event in prostate carcinogenesis. *ERG* rearrangements and *PTEN* loss are frequent and concomitant events in PrCa that cooperate in progression. In addition, *PTEN* and *TP53* tumor suppressor genes are deleted in about 20-40% of PCa and the E3 ubiquitin ligase adaptor speckle-type POZ protein (SPOP) is mutated in about 10% of the samples. SPOP protein targets ERG protein for ubiquitin-proteasome degradation. SPOP is frequently dysregulated in PrCa, either via somatic mutations or mRNA downregulation, suggesting an important tumor suppressor function. Moreover, *SPOP* mutations are associated with an increase in ERG protein levels, but these mutations appear to be mutually exclusive with *ERG* rearrangements in a subset of PrCa.

Objectives

The objective of this study is to analyze the prevalence of *SPOP* alterations in PrCa and to determine the relationship of *SPOP* status, *ERG* rearrangement and *PTEN* loss with the different clinical and pathological variables of prostate cancer.

Material and methods

Tumor Samples and Patients.-

A total of 82 PrCa tumors and 3 benign prostate samples were selected retrospectively from the files of the Parc de Salut MAR Biobank (MARBiobanc), Barcelona, Spain. Frozen samples were available from all cases. According to the ISUP 2016 grading criteria, the Grade Groups (GG) of the tumors were: 1 (n = 14), 2 (n = 20), 3 (n = 16), 4 (n = 16) and 5 (n = 9).

RNA Extraction and Retro-transcription.-

Total RNA was extracted from all 82 frozen prostate tumor samples and the 3 non-tumoral samples. RNA purity and quality were assessed with NanoDrop® (NanoDrop Technologies, USA) and the Agilent 2100 Bioanalyzer (Agilent, USA). cDNA was synthesized using 1μg of total RNA and Superscript II (Invitrogen, Life Technologies Corporation, CA, USA).

SPOP mutational analysis.-

Mutational analysis of *SPOP* hotspot regions (exons 5 and 6) was performed from cDNA in all cases. Primer sequences and PCR conditions are shown in Table 1. Sanger sequencing reactions were done with Big Dye Terminator Kit v.3.1 (Thermo Fisher Scientific MA, USA).

SPOP, TMPRSS2-ERG, ERG and *PTEN* RT-qPCR analysis.-

qPCR was performed from cDNA using TaqMan® Gene Expression Assays (Thermo Fisher Scientific MA, USA). Samples were run in triplicate and non-neoplastic prostate samples were used to normalize the data. Assay Identification for *SPOP, TMPRSS2-ERG, ERG* and *PTEN* were: Hs00737433_m1, Hs03063375_ft, Hs01554629_m1, and Hs02621230_s1, respectively. *GADPH* (4310884E) was used as internal control. *TMPRSS2-ERG* positive rearrangement was considered for 2^(-ΔCt) ≥ 0.0015. *ERG* overexpression for 2^ (-ΔCt) ≥ 0.13, *PTEN* loss for 2^(-ΔCt) < 0.0035, and SPOP loss for 2^(-ΔΔCt) < 0.40.

Table 1. Primer sequences, PCR conditions and *SPOP* mutations found in prostate tumor samples.

PCR CONDITIONS			
SPOP (cDNA)	**Primer sequence**	**Fragment (bp)**	**Temperature**
Exon 5-6 forward	TTGCGAGTAAACCCCAAAGG	271	63°
Exon 5-6 reverse	AAGCTTACCCTCTTCTGCGA	271	63°
MUTATIONAL ANALYSIS			
Exon	**Type of mutation**	**Number of Tumors**	**Grade Group**
5	Y87C	1	2
6	D130V	1	1
6	F133V	1	4
6	F133L	2	3 / 5

Results

TMPRSS2-ERG, ERG, SPOP and *PTEN* quantitative mRNA expression in PrCa.-

Forty-nine (59.8%) and 48 (58.5%) of 82 tumors overexpressed *TMPSS2-ERG* and *ERG* mRNA, respectively. Loss of *SPOP* expression by qPCR was detected in 22 of 82 tumors (26.8%), and *PTEN* loss in 29 of 73 PrCa (39.7%) (Figure 1).

TMPRSS2-ERG, ERG overexpression and *PTEN* loss in PrCa according to Grade Group classification.-

TMPRSS2-ERG rearrangement (p = 0.629), *ERG* overexpression (p = 0.653) and *PTEN* loss (p = 0.427) were not associated with any of the five grade groups. Also, neither the combination *TMPRSS2-ERG/PTEN* loss (p = 0.423) nor *ERG* overexpression/*PTEN* loss (p = 0.425) were associated with any of the five grade groups.

SPOP mutations in Prostate Cancer.-

Five of the 82 (6.1%) prostate tumors showed *SPOP* mutations. Number and type of mutations are shown in Table 1. One of 14 (7.1%) GG1, 1 of 20 (5%) GG2, 1 of 16 (6.3%) GG3, 1 of 16 (6.3%) GG4 and 1 of 9 (11.1%) GG5 tumors harbored mutations in this gene. Examples of *SPOP* mutations are shown in Figure 2.

Relationship of *SPOP* mutations with *TMPRSS2-ERG, ERG* and *PTEN* status.-

SPOP mutations are mutually exclusive with *TMPRSS2-ERG* rearrangement (p = 0.00015) but not with *ERG* overexpression (p =0.154) and *PTEN* expression loss (p = 0.149) (Figure 3A-C).

Relationship of *SPOP* expression loss with *TMPRSS2-ERG, ERG* and *PTEN* status.-

Eighteen of 22 (82%) PrCa with SPOP expression loss harbored a *TMPRSS2-ERG* rearrangement (p = 0.0136), and 17 of 22 (77.3%) overexpressed *ERG* (p = 0.0370) (Figure 4A and B). In addition, 5 of 20 (75%) of tumors with *SPOP* downregulation showed also *PTEN* expression loss (p = 0.00015) (Figure 4C), and 13 of 20 (65%) showed the *ERG*-overexpression/*PTEN*-loss combination (p = 0.0012) (Figure 4D).

SPOP alterations (mutations and expression loss), *ERG* and *PTEN* status and Grade Group classification.-

SPOP alterations, taking together mutations plus expression loss, were more frequent in GG5 (55.5%) than in GG1 to 4 (26.3% to 31.3%) but without statistical significance (p = 0.558) (Figure 5). *ERG+/PTENwt/SPOPwt* phenotype was found in 43% of GG1 and in 18.6% of GG2-5 tumors (p=0.077).

Figure 1. Prevalence of *TMPRSS2-ERG, ERG* overexpression, *SPOP* and *PTEN* expression loss in PrCa.

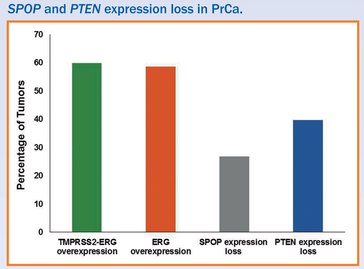

Figure 2. Examples of *SPOP* mutations. #Case 181, Y87C mutation in exon 5. #Case 18, exon 5 *wt*. #Case 183, F133L mutation in exon 6 and #Case 160, exon 6 *wt*.

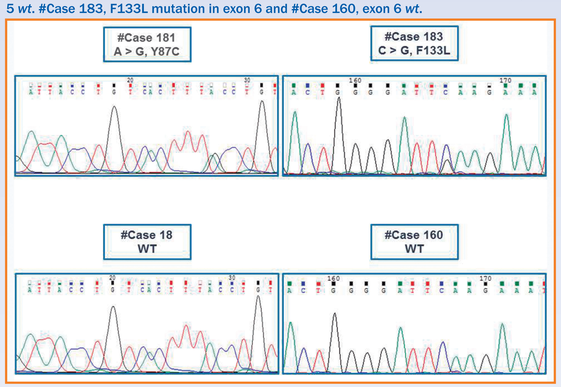

Figure 3. Relationship of *SPOP* mutations with *TMPRSS2-ERG, ERG* and *PTEN* status. *SPOP* mutations are associated with non-rearranged tumors **(A)**. *SPOP* mutation prevalence is higher in *ERG* wt tumors **(B)** and *PTEN* wt tumors **(C)** but without statistical significance.

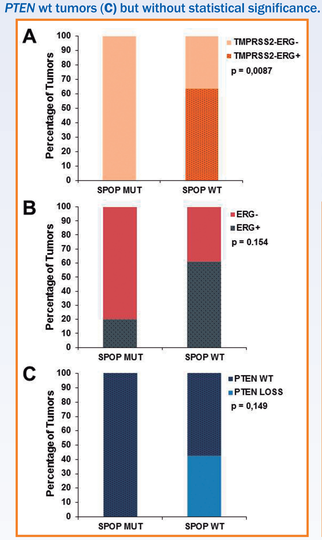

Figure 4. Relationship of SPOP expression loss with *TMPRSS2-ERG, ERG* and *PTEN* status. *SPOP* downregulation was associated with *TMPRSS2-ERG* **(A)** and *ERG* overexpressing tumors **(B)**. *SPOP* downregulation was also associated with *PTEN* loss tumors **(C)**, and with *ERG*-overexpression/*PTEN*-loss combination **(D)**.

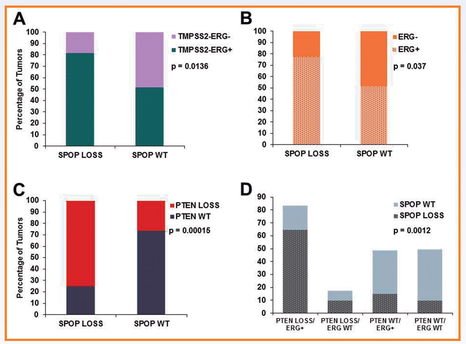

Figure 5. *SPOP* alterations (mutations and expression loss) and Grade Group tumor classification.

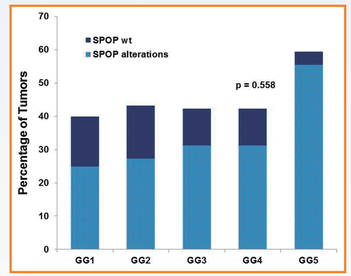

Conclusions

- *SPOP* mutations are mutually exclusive with *TMPRSS2-ERG* rearrangement.
- Loss of *SPOP* expression is associated with *TMPRSS2-ERG, ERG* overexpression, *PTEN* loss and with the *ERG*-overexpression/*PTEN*-loss phenotype.
- *SPOP* alterations (mutations plus expression loss) are more frequent in GG5 than in GG1 to GG4.
- *ERG* overexpression/*PTEN wt/SPOP wt* phenotype shows a trend to be associated with low Grade Group tumors.
- *SPOP* mutations may represent an alternative, *ERG-wt* pathway. However, *SPOP* expression loss is associated with *ERG* fusion and *PTEN* loss in PrCa.

References

- Carver BS, Tran J, Gopalan A, et al. Aberrant ERG expression cooperates with loss of PTEN to promote cancer progression in the prostate. Nat Genet (2009), 41:619-24.
- Berger MF, Lawrence MS, Demichelis F, et al. The genomic complexity of primary human prostate cancer. Nature (2011), 470:214-20.
- Adamo P, Ladomery MR. The oncogene ERG: a key factor in prostate cancer. Oncogene (2016), 35: 403–414.
- Krohn A, Freudenthaler F, Harasimowicz S et al. Heterogeneity and chronology of PTEN deletion and ERG fusion in prostate cancer. Mod Pathol (2014), 27:1612-20.
- Gan W, Dai X, Lunardi A et al. SPOP Promotes Ubiquitination and Degradation of the ERG Oncoprotein to Suppress Prostate Cancer Progression. Mol Cell (2015), 59:917-30.
- Duan S, Pagano M. SPOP Mutations or ERG Rearrangements Result in Enhanced Levels of ERG to Promote Cell Invasion in Prostate Cancer. Mol Cell (2015), 59:883-4.
- Hernández S, Font-Tello A, Juanpere N, et al. Concurrent TMPRSS2-ERG and SLC45A3-ERG rearrangements plus PTEN loss are not found in low grade prostate cancer and define an aggressive tumor subset. Prostate (2016), 76: 854–865.
- Hernández-Llodrà S, Juanpere N, Muga S et al. ERG overexpression plus SLC45A3 (prostein) and PTEN expression loss: Strong association of the triple hit phenotype with an aggressive pathway of prostate cancer progression. Oncotarget. (2017) May 26. doi: 10.18632/oncotarget.

Support Grants:
(FIS/ Carlos III/ FEDER/ PI15/00452, Spanish Ministry of Health).

Hospital del Mar

Parc de Salut MAR Barcelona

Detection of *ALK* and *ROS1* Rearrangements Using Next Generation Sequencing in Lung Cancer: Comparison between FISH, IHC and NGS

Sergi Clavé[1,2], Natalia Rodon[3], Lara Pijuan[1,2], Alba Dalmases[1,2], Olga Díaz[3], Álvaro Taus[2,4], Marta Lorenzo[1,2], Pedro Rocha[2,4], Ana M Muñoz-Mármol[5], Glòria Oliveras[6], Joaquim Bosch-Barrera[6], Blanca Espinet[1,2], Beatriz Bellosillo[1,2], Xavier Puig[3], Edurne Arriola[2,4], and Marta Salido[1,2]

1. Pathology Department, Hospital del Mar, Barcelona, Spain. 2. Cancer Research Program, Hospital del Mar Medical Research Institute (IMIM), Barcelona, Spain.
3. BIOPAT Biopatologia Molecular S.L., Grup Assistència, Barcelona, Spain. 4. Medical Oncology Department, Hospital del Mar, Barcelona, Spain.
5. Pathology Department, Hospital Universitari Germans Trias i Pujol, Badalona, Spain. 6. Medical Oncology Department, Catalan Institute of Oncology (ICO), Girona, Spain.

Disclosures: The authors of this abstract have declared no conflicts of interest.

Contact: sclave@imim.es

BACKGROUND

- Detection of *ALK* and *ROS1* rearrangements in non-small cell lung cancer (NSCLC) is required for directing patient care.
- While fluorescence *in situ* hybridization (FISH) and immunohistochemistry (IHC) have been established as gold standard methods, next generation sequencing (NGS) platforms are called to be at least equally successful, but also more compatible with multiplexing and diagnostic workflows.
- Our aim was to investigate the performance of NGS in the detection of rearranged cases.

DESIGN

Forty-two NSCLC samples were selected retrospectively from our database (n= 3.360) based on previous *ALK* (n= 34) and *ROS1* (n= 8) FISH results (positive or inconclusive) and material availability **(Figure 1)**.
Cases were tested by both FISH (Abbott Molecular) and IHC (Ventana) in paraffin blocks, and were reviewed centrally to determine the tumor area. DNA and RNA were manually extracted from paraffin sections. Ion Torrent sequencing technology with Oncomine™ Focus Assay (Thermo Fisher Scientific) were applied using 10ng DNA and 100ng RNA from each sample **(Figure 2)**.

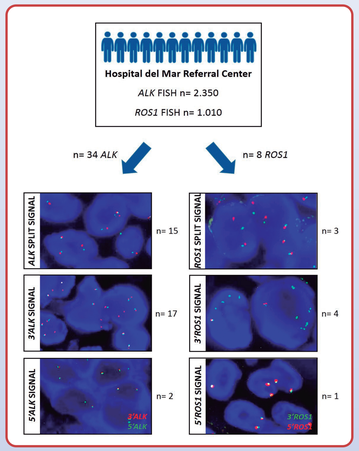

Figure 1. Sample collection. Our Institution has been testing NSCLC samples as a referral center since 2011. We screened all samples by FISH with break-apart probes.

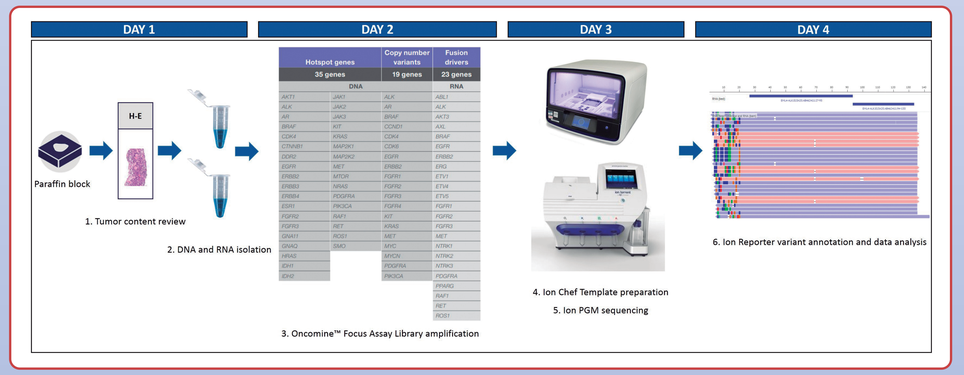

Figure 2. Oncomine™ Focus Assay workflow. Paraffin blocks were re-evaluated to ensure the minimum tumor area and percentage of infiltration. DNA and RNA were isolated using RecoverAll Total Nucleic Acid Isolation Kit for FFPE and 10ng DNA and 100ng RNA were used to perform Oncomine™ Focus Assay (Thermo Fisher Scientific).

RESULTS

Patient's characteristics were median age 60 years, 52% males, and 83% diagnosed as adenocarcinoma (ADC).
Regarding FISH results, 18 cases had split signals, 21 had isolated 3' signals, and three had negative FISH pattern with isolated 5' signals **(Figure 1)**. Testing with IHC, nine out of the 42 cases were negative: the three isolated 5' FISH negative and six isolated 3' FISH positive cases (discordance FISH vs. IHC) **(Figure 3)**.
NGS technology detected positive *ALK* and *ROS1* fusions in 82% of the assessable samples (27/33), being *EML4*(13)-*ALK*(20) and *EZR*(10)-*ROS1*(34) the most prevalent **(Figure 4)**.
Nine cases (21%) were non-evaluable by NGS due to insufficient sequencing coverage (seven were small biopsies with low RNA input).
Regarding the six cases with negative NGS result: three were the isolated 5' FISH negative cases in accordance with negative IHC, and the other three presented isolated 3' FISH positive pattern, negative by IHC (**Figure 5**).

FISH				FISH				IHC		
IHC	SPLIT	3'	5'	NGS	SPLIT	3'	5'	NGS	POS	NEG
POS	18	15	0	POS	15	12	0	POS	27	0
NEG	0	6	3	NEG	0	3	3	NEG	0	6
				FAIL	3	6	0	FAIL	6	3

Figure 3. Comparison between FISH, IHC and NGS. Cases with *ALK* or *ROS1* positive FISH split signals were all positive by IHC and NGS. Discordant cases were restricted to those considered FISH positive with 3' isolated signals.

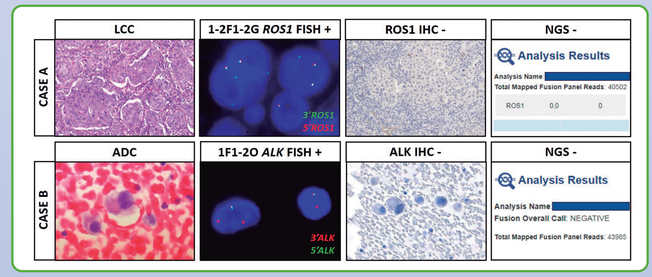

Figure 5. Discordant 3' isolated FISH positive cases. These cases potentially indicate a FISH false-positive result caused by non-productive rearrangements. Both IHC and NGS are valid alternative tests to check these alterations.

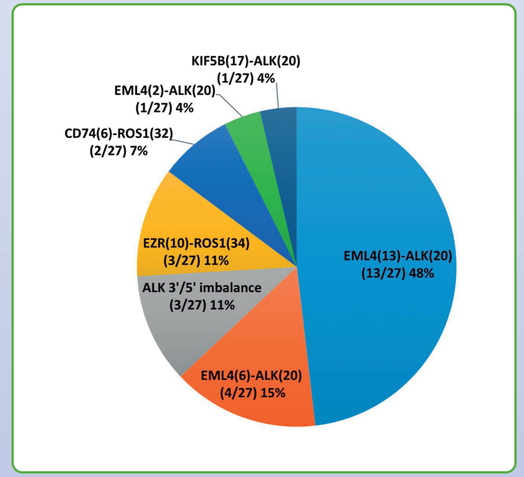

Figure 4. Fusion gene frequency. In agreement with previous series, *EML4*(13)-*ALK*(20) and *EZR*(10)-*ROS1*(34) fusions were the most prevalent. Remarkably, there were three *ALK* rearranged cases without partner defined (imbalance 3'/5').

CONCLUSIONS

- NGS technology for detecting *ALK* and *ROS1* rearrangements in NSCLC could be considered as a screening test although the success rate is closely related to the correct evaluation of the initial amount of tumor tissue, particularly in small biopsies.
- The discordance observed in the isolated 3' FISH positive cases potentially indicates that this alteration could be a FISH false-positive result.
- NGS technology could be used as an additional molecular technique for cases with inconclusive or discordant FISH/IHC results.

Hospital del Mar
Parc de Salut MAR Barcelona